International Journal of Mass Spectrometry 481 (2022) 116913

Contents lists available at ScienceDirect

International Journal of Mass Spectrometry

journal homepage: www.elsevier.com/locate/ijms

# Rapid identification of short oligonucleotide impurities using lithium adduct consolidated MALDI-TOF mass spectrometry

Owen B. Becette [a], Anh Tran [b], John P. Marino [a], Jace W. Jones [b, **], Robert G. Brinson [a, *]

[a] Institute for Bioscience and Biotechnology Research, National Institute of Standards and Technology and the University of Maryland, 9600 Gudelsky Drive, Rockville, MD, 20850, United States
[b] Department of Pharmaceutical Sciences, University of Maryland School of Pharmacy, Baltimore, MD, 21201, United States

ARTICLE INFO

*Article history:*
Received 2 March 2022
Received in revised form
20 July 2022
Accepted 29 July 2022
Available online 8 August 2022

*Keywords:*
MALDI-TOF MS
NMR
RNA
Product impurities
Quality attributes

ABSTRACT

Nucleic acids are an increasingly popular platform for the development of pharmaceuticals to treat and prevent multiple diseases including those where traditional small molecule and protein-based drug development efforts have failed. Short oligonucleotide therapeutics, which consist of antisense oligonucleotides (ASOs) and short interfering ribonucleic acids (siRNAs), are prepared by solid phase chemical synthesis, which can generate various impuriies that have the potential to lower drug safety and efficacy. Drug substance-related impurities can be especially difficult to identify and characterize. To address this short coming, here we apply lithium adduct consolidation with matrix-assisted laser desorption/ionization (MALDI) time-of-flight (TOF) mass spectrometry (MS) to afford a simplified, quick, and facile method for identification of a known drug substance impurity, isobutyryl (iBu) groups arising from incomplete deprotection during solid phase synthesis. We further employ high-resolution nuclear magnetic resonance (NMR) spectroscopy to confirm assessment of the iBu impurity. This lithium adduction consolidation method should find general applicability for routine quality assessment of synthetic oligonucleotides in both academic and industrial laboratories.



## 1. Introduction

Short oligonucleotide therapeutics are an emerging class of biopharmaceuticals to treat and prevent a wide variety of human diseases, including those deemed “undruggable” by traditional small molecule and protein-based drug platforms [1–3]. In contrast to native nucleic acids, which are prepared enzymatically with polymerases, short oligonucleotides are prepared chemically via solid phase chemical synthesis [4,5]. Solid phase chemical synthesis provides a facile approach for incorporation chemical modifications, including 2′-fluoro (2′-F) and 2′-*O*-methyl (2′-OMe) groups, introduced during drug development to overcome the poor pharmacological properties of native nucleic acids [2,3]. During solid phase chemical synthesis, the reactive groups on adenosine (A), cytosine (C), guanine (G), and uridine (U) nucleosides are protected to prevent unwanted side reactions that lower yields and introduce impurities. The reactive 2′-hydroxyls are rendered inert most commonly with *tert*-butyldimethylsilyl groups (TBDMS) while the amino groups are traditionally protected with acetyl (Ac), phenoxyacetyl (Pac), benzoyl (Bz), and isobutyryl (iBu) groups [5]. Upon termination of the synthesis, the oligonucleotides are cleaved from the solid support and deprotected. During the solid phase chemical synthesis and subsequent deprotection reactions, multiple impurities are potentially generated that require identification and quantification prior to downstream applications [6,7].

Here we demonstrate a MALDI-TOF MS method to identify an iBu-protected siRNA impurity resulting from the incomplete deprotection of our model siRNA (Fig. 1). In particular, we apply LiCl enrichment to promote lithium adduct consolidation and significantly reduce the presence $Na^+$ and $K^+$ adducts, a technique commonly applied to lipids [8,9]. This protocol reduced variability, greatly facilitating interpretation of the mass spectrum. Coupled with supporting high-resolution NMR analysis, we show how MS and NMR methods can be applied synergistically to identify

* Corresponding author. Institute for Bioscience and Biotechnology Research National Institute of Standards and Technology 9600 Gudelsky Drive Rockville, Maryland, 20850, United States.
** Corresponding author. Department of Pharmaceutical Sciences, University of Maryland School of Pharmacy, 20 N. Pine Street, Room N721, Baltimore, MD 21201, United States.
*E-mail addresses:* jjones@rx.umaryland.edu (J.W. Jones), robert.brinson@nist.gov (R.G. Brinson).

https://doi.org/10.1016/j.ijms.2022.116913
1387-3806/

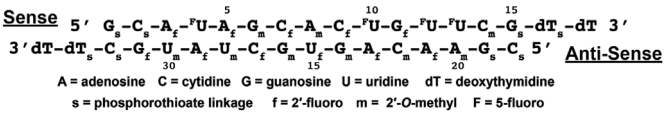


**Fig. 1.** The sequence and secondary structure scheme of the model siRNA.

oligonucleotide impurities in a manner that has broad applicability to this therapeutic platform. Importantly, the iBu-protected siRNA impurity evaded detection by commonly used low-resolution analytical techniques, including polyacrylamide gel electrophoresis (PAGE) and fast protein liquid chromatography (FPLC) analyses, thereby necessitating the demand for higher resolution methods.

## 2. Methods

### 2.1. Samples

The model siRNA was purchased from two different vendors (V), herein referred to as V1 and V2. Due to production problems with V2, the identities of the two vendors will be kept anonymous. The V1 siRNA was purchased as a duplex, was previously well-characterized by NMR and MS [10], and is presented here only as a control. The V2 siRNA was supplied as antisense (AS) and sense (S) strands. The V2 siRNA was obtained from two separate 0.5 μmol−2 μmol syntheses of each strand (AS and S). The siRNAs were provided as crude products and required purification prior to any MALDI-TOF MS or NMR analysis.

### 2.2. PAGE purification

Large scale PAGE purification of the individual RNA strands were performed as described previously [10]. Briefly, gels were cast with approximately 200 mL (plate dimensions: 45 cm × 30 cm x 0.15 cm) of 20% acrylamide:bis (19:1), 8 M urea, with 1 X TBE (90 mM tris-borate pH 8.3, 2 mM EDTA) as the running buffer. The gels were polymerized by the addition of 1 mL 10 mg/mL ammonium persulfate (APS) and 50 μL tetramethylethylenediamine (TEMED). Approximately 0.5 μmol−1 μmol of each oligonucleotide (AS and S) was dissolved in 0.5 mL 8 M urea, 1 X TBE and 0.5 mL 2 X formamide loading dye (80% formamide, 50 mM EDTA, 10% glycerol, 0.025% bromophenol blue). The gels ran overnight at 10 W after which the RNAs were visualized by UV shadowing, excised with ethanol-soaked razor blades, and eluted from the gel in 0.5 X TBE using a Whatman Elutrap™ electroelution system (GE Healthcare, Chicago, IL). The oligonucleotides were successively exchanged into de-ionized 18.2 MΩ water (twice), 1 M NaCl (once), and de-ionized 18.2 MΩ water (thrice) using 4-mL 3 kDa centrifugal filters (Millipore-Sigma, Burlington, MA). The oligonucleotide purity was confirmed by analytical PAGE, which shows a single homogenous band following large-scale purification (Fig. S1). As a control sequence, an abasic version of the sense strand (*S) was loaded. The AS and S strands were mixed in a 1:1 M ratio, denatured at 95 °C for 2 min, then annealed by slow cooling to give the duplex siRNA. The V2 siRNA was exchanged five times into formulation buffer (10 mM sodium phosphate pH 6.5, 50 mM sodium chloride, 0.02% sodium azide, 0.1 mM sodium trimethylsilylpropanesulfonate (DSS-d6), 5% $D_2O$) and concentrated using a 0.5-mL 3 kDa centrifugal filter (Millipore-Sigma, Burlington, MA). The chosen formulation buffer are common components of short oligonucleotide drug formulations [10,13,14]. A 300 μL aliquot (0.5 mM siRNA) was transferred to a 5 mm Shigemi tube (Cortecnet, Brooklyn, NY) for NMR analysis.

### 2.3. Purification by liquid chromatography

Approximately 150 nmol batches of the V1/V2 siRNAs were applied to a MonoQ™ 5/50 GL column (GE Healthcare, Chicago, IL) equilibrated with 20 mM sodium phosphate pH 6.5 and eluted over 40 column volumes (CV = 1 mL) with a linear gradient from 0 M−1 M NaCl and a 2 mL/min flow rate. The absorbance at λ = 260 nm was monitored as a function of elution volume on a Äkta™ FPLC Purifier (GE Healthcare, Chicago, IL) (Fig. S2). The FPLC trace of the V2 siRNA purification was consistent with the V1 siRNA chromatogram published previously [10]. The fractions containing the siRNA (0.5 mL each) were pooled, concentrated, and exchanged three times into de-ionized 18.2 MΩ water using 4-mL 3 kDa centrifugal filters. The siRNAs were then exchanged five times into formulation buffer and concentrated to 300 μL in 0.5-mL 3 kDa centrifugal filters. An aliquot of the V2 siRNA was further purified by AEX (AEX V2 siRNA, 0.5 mM) to remove any residual acrylamide contamination from the PAGE purification process [15,16].

### 2.4. MALDI-TOF MS acquisition and analysis

The model siRNA was precipitated with 1.5 M ammonium acetate in ethanol at −20 °C to strip metal ions (*e.g.*, $Na^+$ and $K^+$) from the nucleic acid backbone prior to MALDI-TOF MS analysis [10,17]. 0.5 μL of approximately 100 μM siRNA was co-spotted with 0.5 μL LiCl solution (0.0, 1.5, or 6.0 mg/mL LiCl in 1:1 acetonitrile:water) and 1 μL 3-HPA matrix (0.7 M 3-hydroxypicolinic acid, 0.05 M ammonium citrate tribasic, 0.1% trifluoroacetic acid in 1:1 acetonitrile:water) with the dried-droplet spotting technique. The same procedure was used to test the applicability of ammonium enrichment with 0.5 μL of the same molar equivalent of $NH_4Cl$ (1.9 mg/mL) in place of LiCl. The data were collected in positive reflectron and negative reflectron mode using a microfleX MALDI-TOF mass spectrometer (Bruker, Billerica, MA) on samples spotted on an MSP 96 ground steel plate (Bruker, Billerica, MA). A laser frequency of 60 Hz for 100 shots per sample was used with random walk mode enabled. The *m/z* range was set to 2000 Da−8000 Da in low mass range mode. Mass calibration of the TOF was done in the range of 3500 *m/z* to 7500 *m/z* using SpheriCal™ High Peptide MALDI-MS calibration kit (Polymer Factory, Stockholm, Sweden). All data were analyzed via Bruker's flexAnalysis software (Billerica, MA).

### 2.5. Analytical PAGE

The oligonucleotide purity was assessed by analytical PAGE performed on gels cast with approximately 10 mL of 20% acrylamide:bis (19:1), 8 M urea with 1 X TBE as the running buffer. The gels were polymerized with 100 μL 10 mg/mL APS and 5 μL TEMED. Each oligonucleotide was mixed with an equal volume of 2 X formamide loading dye and denatured at 95 °C for 5 min 5 μL of the crude and purified oligonucleotides were loaded onto the gel. The oligonucleotides were resolved with the application of 200 V for approximately 1 h and visualized with ethidium bromide (1 μg/mL) staining.

### 2.6. NMR data acquisition and processing

1D $^1H$ and 2D $^1H$–$^1H$, $^1H$–$^{13}C$ NMR measurements were collected on a 600 MHz Bruker Avance III spectrometer (Billerica, MA) equipped with actively shielded z-axis gradient triple resonance TCI cryoprobe. All samples were prepared under typical formulation conditions and spiked with 5% $D_2O$ for a field-frequency lock and 0.1 mM DSS-d6 as an internal reference. All measurements were performed in water (5% $D_2O$/95% $H_2O$) at 15 °C

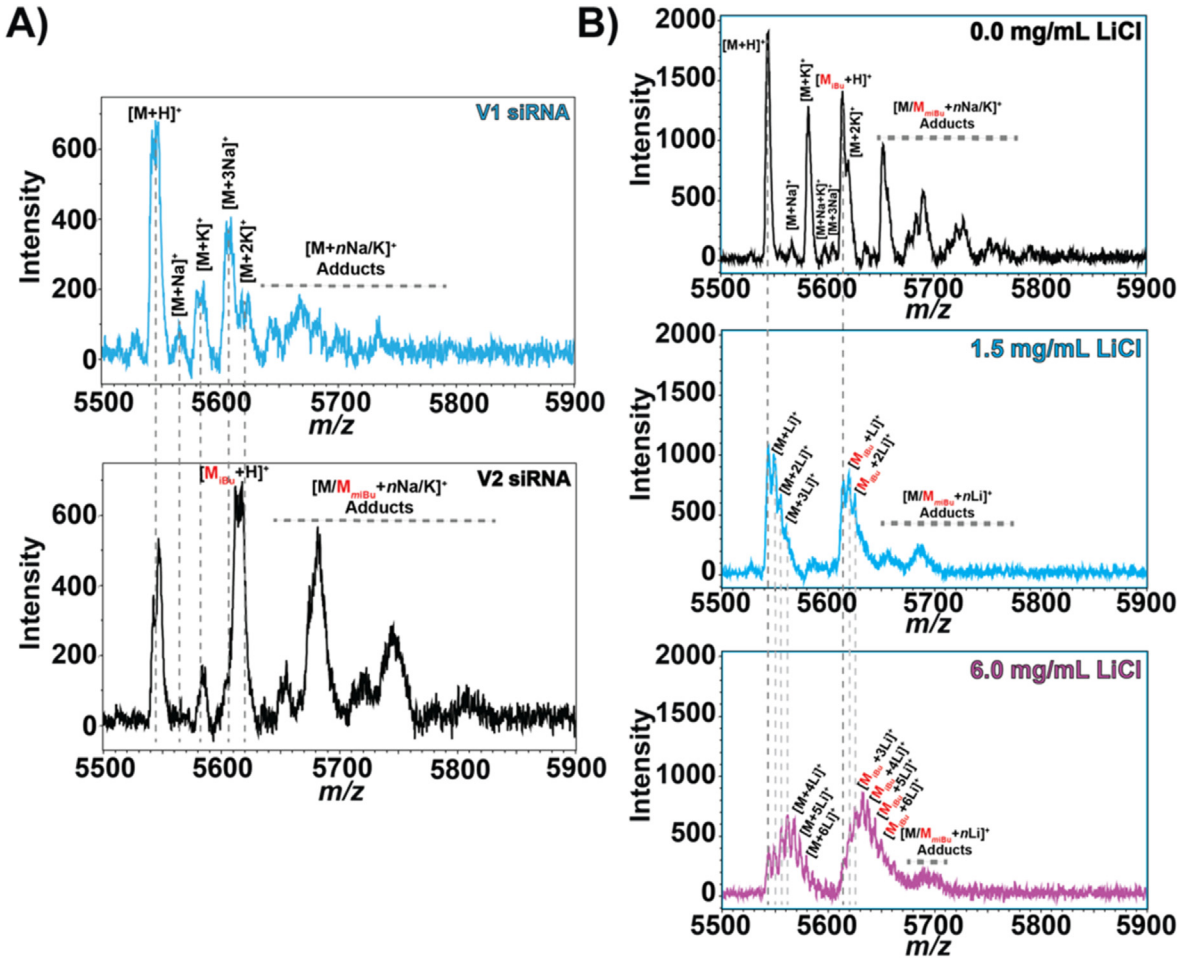


**Fig. 2.** MALDI-TOF MS of the siRNAs from vendor 1 (V1) and vendor 2 (V2) collected in positive reflectron mode. **A**) V1 siRNA (cyan, top panel) and V2 siRNA (black, bottom panel) samples, both without lithium chloride. **B**) V2 sense (S) siRNA co-spotted with 0.0 mg/mL (black, top panel), 1.5 mg/mL (cyan, middle panel), and 6.0 mg/mL (magenta, bottom panel) LiCl in 1:1 acetonitrile:water. The $H^+$, $Li^+$, $Na^+$, and $K^+$ adducts are notated along with the fully deprotected and iBu protected *m/z* values (M and $M_{iBu}$). See Methods section for detailed sample preparation and experimental conditions.

**Table 1**
Limit of Detection assessment of protonated adducts from LiCl addition. The ratio of the $[M+H]^+$ and $[MiBu + H]^+$ adduct S/N values in the absence of LiCl enrichment was used to calculate the approximate amount of each species (M: 57%, 28.5 pmol; MiBu: 43%, 21.5 pmol).

| LiCl (mg/mL) | Adduct (S/N) | | LOD |
|---|---|---|---|
| | [M+H]+ | [MiBu + H]+ | (pmol) |
| 0.0 | 48.8 | 36.6 | 1.8 |
| 1.5 | 26.9 | 19.9 | 3.2 |
| 3.0 | 10.6 | 9.1 | 7.6 |
| 6.0 | 6.6 | 6.0 | 11.9 |

LOD = limit of detection.

and 25 °C for exchangeable and non-exchangeable $^1H$ measurements, respectively. Solvent suppression was achieved via water flip-back [18] and WATERGATE [19]. 1D $^1H$ data were collected with 8 scans, 200 ms acquisition times, and a 2 s interscan delay in a total measurement time of less than 30 s 2D $^1H-^{13}C$ HSQC spectra were collected in 4 h with 128 scans per $t_1$ increment, 140 ms and 9.4 ms acquisition times in $^1H$ ($t_2$) and $^{13}C$ ($t_1$) dimensions, respectively, 50% non-uniform sampling (NUS) [20], and a 1.5 s recycle delay. 2D $^1H-^1H$ NOESY data were recorded with 32 scans, 140 ms ($t_2$) and 26 ms ($t_1$) acquisition times, 100 ms mixing time ($t_{mix}$), and a 1.5 s relaxation delay for a total experiment time of approximately 8 h $^1H$ chemical shifts were internally referenced to DSS (0.00 ppm) and $^{13}C$ using the frequency ratio $^{13}C/^1H = 0.251449530$, where $^1H$ refers to the frequency of the internal DSS signal [21]. All data were collected in Topspin (Bruker, Billerica, MA), processed with NMRPipe [22], and analyzed with NMRView [23]. NUS spectra were reconstructed in NMRPipe using the iterative soft thresholding (IST) method [24].

## 3. Results and discussion

MS analysis of oligonucleotides is complicated by their polyanionic nature, which makes them ideal for negative ion mode detection but also prone to the formation of adducts containing sodium and potassium, which reduces mass accuracy, increases variability, and increases mass spectral complexity [7]. Further complicating the analysis is the presence of both strands (AS and S) of the siRNA, which have *m/z* values that differ by only 5 Da, with measured values of S: 5546.688 *m/z*; AS: 5541.729 *m/z*) [10]. We therefore analyzed both the intact siRNA as well as individual strands separately by MALDI-TOF MS (Fig. 2, S3). Both negative- and positive-ion modes showed the sodiated and potassiated adducts, but positive-ion mode gave better signal-to-noise (approximately 10-fold higher) and was therefore used for the subsequent analysis (Fig. 2, S3, S4, S5). Analysis of the V2 siRNA sample by MALDI-TOF

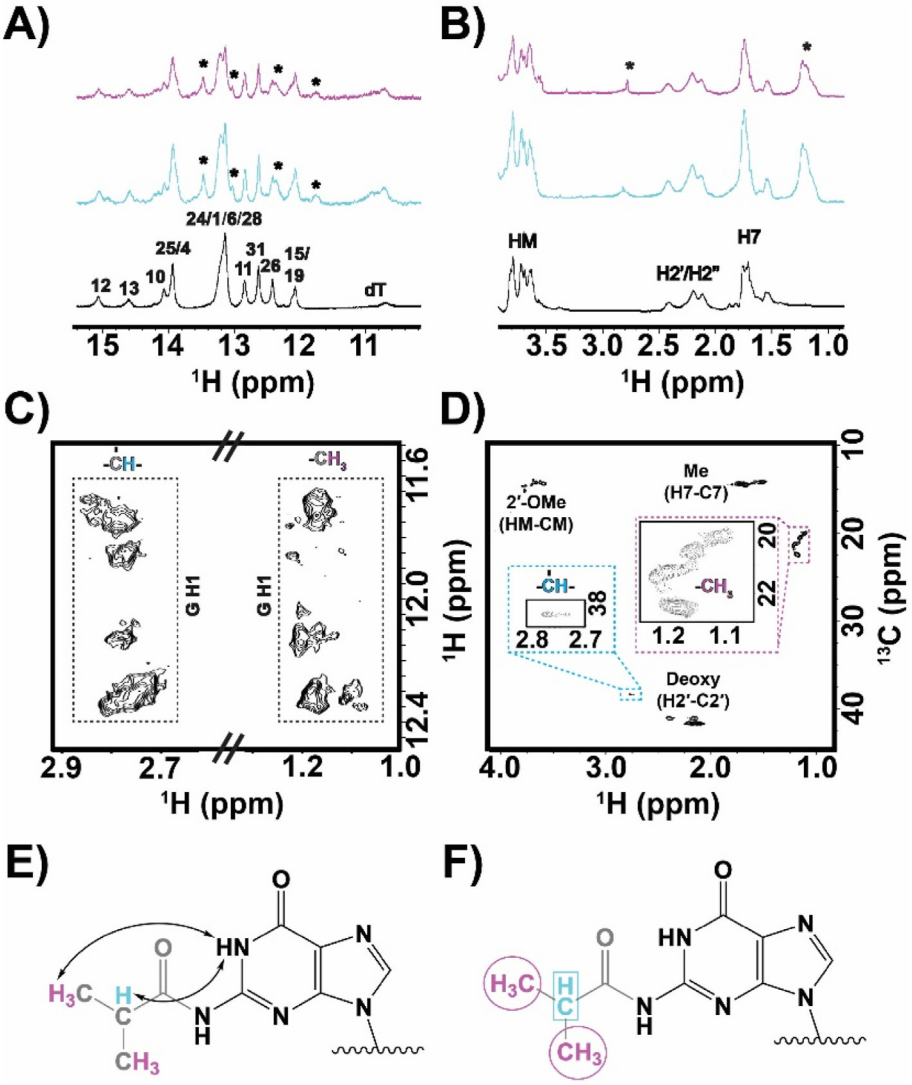


**Fig. 3.** NMR data collected at 600 MHz on the siRNA samples purchased from different vendors. **A)** The imino region and **B)** aliphatic region of the 1D $^{1}$H spectra of the vendor 1 (V1, black), vendor 2 (V2, cyan), and anion-exchange purified V2 (V2 AEX, magenta) samples, recorded at 15 °C. The imino $^{1}$H assignments, published previously [10], are shown for the V1 siRNA. The additional $^{1}$H signals in Panels **A** and **B** are denoted by black asterisks. To account for the differences in sample concentrations, the V2 and V2 AEX signal intensities are scaled 4 times higher than the V1 siRNA. **C)** The imino-aliphatic region of the 2D $^{1}$H−$^{1}$H NOESY collected on the V2 siRNA at 15 °C. Boxed regions highlight the imino − methine and imino − methyl contacts. **D)** The aliphatic region of the 2D $^{1}$H−$^{13}$C HSQC collected on the V2 siRNA at 25 °C. Boxed regions are close-ups of the methine (cyan) and methyl (magenta) regions. **E)** The observed NOEs from Panel **C** are illustrated on an N2-isobutyrylguanosine. **F)** The methyl and methine $^{1}$H−$^{13}$C correlations shown in **D)** are depicted on an N2-isobutyrylguanosine. For all panels, full experimental details are given in the Methods section.

MS afforded a mass spectrum that could not be fully explained by $Na^+$ and $K^+$ adducts (Fig. 2, S3, S4). Further enriching the samples with ammonium by co-spotting with $NH_4Cl$ had negligible impact on the removal on the $Na^+$ and $K^+$ adducts (Fig. S5). These salt adducts were present despite extensive desalting and ethanol precipitation with ammonium acetate and the presence of ammonium citrate in the MALDI matrix [10,17]. In principle, ammonium ($NH_4^+$) replaces bound $Na^+$ and $K^+$ ions from the oligonucleotide and, during ionization, releases ammonia in the gas phase while leaving protons ($H^+$) as counterions [7,17]. However, we observed low repeatability of the mass spectrum, with varying intensities of the salt adducts (Fig. S6). Furthermore, the coefficient of variation (CV) for the $Na^+/K^+$ adducts are highly variable (25%–78%), highlighting the low repeatability of the MALDI-TOF MS data (Fig. S6).

To reduce spectral complexity and variability from the multiple sodiated and potassiated adducts, LiCl was co-spotted onto the plate on top of the siRNA samples, in a manner similar to what has been reported for lipid analysis [8,9]. By doping the siRNA samples with LiCl, presumably any contaminating $Na^+$ and $K^+$ ions are displaced from the nucleic acid by $Li^+$ due to the latter's higher binding affinity [25–27]. While the $Na^+$ and $K^+$ adducts were minimized by this $Li^+$ enrichment, another impurity could now clearly be observed with an *m/z* value 71 Da larger than the $[M+H]^+$ ion, and which is of similar mass of the $[M+3Na]^+$ and $[M+2K]^+$ species (Fig. 2B). The broadness of the *m/z* signal partially obscured the presence of this +71 Da ion species in the non-LiCl-doped mass spectrum due to overlap with the signal from the [M+3Na]+ and $[M+2K]^+$ species (Fig. 2, S3, S4, S5).This signal overlap in the non-LiCl-doped mass spectrum made it difficult to distinguish the +71 Da ion species from the $[M+2K]^+$ species. By co-spotting the V2 siRNA samples with LiCl solutions (1.5 mg/mL to 6 mg/mL LiCl), the $Na^+/K^+$ ions were displaced from the oligonucleotide, which resulted in the consolidation to the $Li^+$ adducts ($[M + nLi]^+$,

where $n = 1, 2, 3$, etc.) and therefore a simplified mass spectrum for interpretation, and only the $[M+H]^+$ and lithiated adducts are present. The *m/z* signal of +71 Da is consistent with the iBu-protected impurity. The signals within each peak cluster are separated by 6 Da, which is consistent with consecutive additions of lithium. Further, the number of lithium adducts increases with LiCl concentrations (Fig. 2B), although this also lowers the signal-to-noise ratio (S/N) and decreases the limit of detection (LOD) for the protonated adduct (Table 1). Overall, the LOD decreased from 3.5 pmol at 0.0 mg/mL LiCl down to 24 pmol at 6.0 mg/mL LiCl. For the case of 6.0 mg/mL LiCl addition, the signal is clearly broadened by multiple lithiated adducts, but the spectral envelope of the $[M + nLi]^+$ species maintains an overall high S/N, if each individual adduct is summed (Table S1). However, in practice, adding less LiCl (*e.g.*, 1.5 mg/mL, Fig. 2B) may prove to be more beneficial for routine use; this amount replaces the majority of sodiated an potassiated adducts, leading to less variability while maintaining intensity of the protonated adduct. Lithium adduct consolidation has been used to characterize lipids by MS [8,9] but to our knowledge has never before been applied to nucleic acids.

To confirm the nature of the impurity, further analysis was undertaken by PAGE and high-resolution NMR. Analytical PAGE suggested that the V2 siRNA sample was pure following large-scale purification, as is evident by a homogenous band for each strand (Fig. S1). However, 1D and 2D NMR analyses confirmed the iBu-protected impurity (Fig. 3). Compared to the previously published data on the V1 siRNA [10], the V2 siRNA contains additional signals in the imino (10 ppm−15 ppm) and aliphatic (1 ppm−3 ppm) regions of the 1D $^1$H spectrum (Fig. 3A and B). The iminos (G H1 and U H3) report on hydrogen bonding, with the number of imino $^1$H signals directly proportional to the number of base-pairs in the siRNA. The extra imino $^1$H signals suggest that there are alternative base-pair structures and/or chemical compositions in the V2 siRNA compared to the control V1 sample. Since the additional aliphatic $^1$Hs at 1.17 ppm and 2.78 ppm are not in the control V1 siRNA, they are most likely arising from the contaminant in the V2 siRNA. 2D $^1$H−$^1$H NOESY data collected on the V2 siRNA suggest that the contaminant is located on the Watson-Crick face of several G residues, as evidenced by the cross-peaks between the additional imino and aliphatic $^1$H signals (Fig. 3C). The impurity was further characterized by 2D $^1$H−$^{13}$C HSQC, which showed two cross-peaks centered at $^1$H: 1.17 ppm/$^{13}$C: 21.4 ppm and $^1$H: 2.78 ppm/$^{13}$C: 38.3 ppm, which are consistent with a methyl and methine group of one or more iBu groups (Fig. 3D). In general, iBu groups are particularly challenging to remove and are common sources of oligonucleotide impurities [7,28−31].

## 4. Conclusion

As short oligonucleotides are manufactured via solid phase chemical synthesis, these therapeutics have been regulated more similarly to small molecules than biologics, despite their larger size and more complex structure. While there is a lack of clear regulatory guidelines for oligonucleotide therapeutics, it is apparent that the overall integrity and purity of short oligonucleotides is essential for drug safety and efficacy [6]. Therefore, practical methods for quick routine assessment of the product-related impurity profile of short oligonucleotides is needed. To this end, we have presented a robust MALDI-TOF MS method to identify product impurities that were not detected by commonly used albeit low resolution laboratory techniques. The method involved a known technique of lithium adduct consolidation to effectively displace sodiated and potassiated adducts with lithiated adducts, which afforded spectra with reduced complexity and decreased variability. The LiCl enrichment facilitated spectral interpretation and allowed for easier identification of an impurity with a mass of 71 Da greater than the fully deprotected siRNA, which is consistent with an iBu group that is used as a protecting group during solid phase synthesis of short oligonucleotides. Additional characterization conducted by 1D and 2D NMR spectroscopy confirmed the identity of this contaminant. Taken together, these results demonstrate that the V2 siRNA sample contains the fully deprotected siRNA as well as an iBu-protected siRNA impurity resulting from incomplete deprotection during its manufacturing, and that this impurity impacts the siRNA structure.

## CRediT authorship contribution statement

**Owen B. Becette:** Conceptualization, Methodology, Investigation, Formal Analysis, Writing − original draft. **Anh Tran:** Investigation, Validation, Writing − Review & Editing. **John P. Marino:** Methodology, Writing − Review & Editing. **Jace W. Jones:** Methodology, Validation, Writing − Review & Editing. **Robert G. Brinson:** Methodology, Project Administration, Supervision, Writing − original draft.

## Disclaimer

Certain commercial equipment, instruments, and materials are identified in this paper in order to specify the experimental procedure. Such identification does not imply recommendation or endorsement by the National Institute of Standards and Technology, nor does it imply that the material or equipment identified is necessarily the best available for the purpose.

## Declaration of competing interest

The authors declare that they have no known competing financial interests or personal relationships that could have appeared to influence the work reported in this paper.

## Acknowledgement

JWJ acknowledges the University of Maryland School of Pharmacy Faculty Start-up funds and the University of Maryland School of Pharmacy Mass Spectrometry Center (SOP1841-IQB2014). AT was partially supported by the Chemistry/Biology Interface (CBI) NIGMS/NIH T32 GM066706. OBB, RGB, and JPM acknowledge the financial support from the NIST Biomanufacturing Program. The authors would also like to thank Dr. William O'Dell for his helpful comments and suggestions.

## Appendix A. Supplementary data

Supplementary data to this article can be found online at https://doi.org/10.1016/j.ijms.2022.116913.

## References

[1] H. Xiong, R.N. Veedu, S.D. Diermeier, Recent advances in oligonucleotide therapeutics in oncology, Int. J. Mol. Sci. 22 (2021) 3295.
[2] J. Lieberman, Tapping the RNA world for therapeutics, Nat. Struct. Mol. Biol. 25 (2018) 357−364.
[3] T.C. Roberts, R. Langer, M.J.A. Wood, Advances in oligonucleotide drug delivery, Nat. Rev. Drug Discov. 19 (2020) 673−694.
[4] S.L. Beaucage, M.H. Caruthers, Deoxynucleoside phosphoramidites—a new class of key intermediates for deoxypolynucleotide synthesis, Tetrahedron Lett. 22 (1981) 1859−1862.
[5] O. Becette, L.T. Olenginski, T.K. Dayie, Solid-phase chemical synthesis of stable isotope-labeled RNA to aid structure and dynamics studies by NMR spectroscopy, Molecules 24 (2019).
[6] D. Capaldi, A. Teasdale, S. Henry, N. Akhtar, C. Den Besten, S. Gao-Sheridan, M. Kretschmer, N. Sharpe, B. Andrews, B. Burm, J. Foy, Impurities in

oligonucleotide drug substances and drug products, Nucleic Acid Therapeut. 27 (2017) 309–322.
[7] S. Pourshahian, Therapeutic oligonucleotides, impurities, degradants, and their characterization by mass spectrometry, Mass Spectrom. Rev. 40 (2021) 75–109.
[8] A. Tran, L. Wan, Z. Xu, J.M. Haro, B. Li, J.W. Jones, Lithium hydroxide hydrolysis combined with MALDI-TOF mass spectrometry for rapid sphingolipid detection, J. Am. Soc. Mass Spectrom. 32 (2021) 289–300.
[9] C.D. Cerruti, D. Touboul, V. Guérineau, V.W. Petit, O. Laprévote, A. Brunelle, MALDI imaging mass spectrometry of lipids by adding lithium salts to the matrix solution, Anal. Bioanal. Chem. 401 (2011) 75–87.
[10] O.B. Becette, A. Tran, J.W. Jones, R.G. Brinson, Structural fingerprinting of siRNA therapeutics by solution NMR spectroscopy, Nucleic Acid Therapeut. 32 (4) (2021) 267–279, https://doi.org/10.1089/nat.2021.0098.
[13] J. Muslehiddinoglu, R. Simler, M.L. Hill, C. Mueller, J.H.A. Amery, L. Dixon, A. Watson, K. Storch, C. Gazziola, F. Gielen, S.A. Lange, J.D. Prail, D.P. Nesta, Technical considerations for use of oligonucleotide solution API, Nucleic Acid Therapeut. 30 (2020) 189–197.
[14] J. Poecheim, K.A. Graeser, J. Hoernschemeyer, G. Becker, K. Storch, M. Printz, Development of stable liquid formulations for oligonucleotides, Eur. J. Pharm. Biopharm. 129 (2018) 80–87.
[15] P.J. Lukavsky, J.D. Puglisi, Large-scale preparation and purification of polyacrylamide-free RNA oligonucleotides, RNA 10 (2004) 889–893.
[16] I. Kim, S.A. Mckenna, E.V. Puglisi, J.D. Puglisi, Rapid purification of RNAs using fast performance liquid chromatography (FPLC), RNA 13 (2007) 289–294.
[17] S. Shah, S.H. Friedman, An ESI-MS method for characterization of native and modified oligonucleotides used for RNA interference and other biological applications, Nat. Protoc. 3 (2008) 351–356.
[18] S. Grzesiek, A. Bax, The importance of not saturating water in protein NMR. Application to sensitivity enhancement and NOE measurements, J. Am. Chem. Soc. 115 (1993) 12593–12594.
[19] M. Piotto, V. Saudek, V. Sklenář, Gradient-tailored excitation for single-quantum NMR spectroscopy of aqueous solutions, J. Biomol. NMR 2 (1992) 661–665.
[20] S. Robson, H. Arthanari, S.G. Hyberts, G. Wagner, Nonuniform sampling for NMR spectroscopy, Methods Enzymol. 614 (2019) 263–291.
[21] D.S. Wishart, C.G. Bigam, J. Yao, F. Abildgaard, H.J. Dyson, E. Oldfield, J.L. Markley, B.D. Sykes, $^{1}H$, $^{13}C$ and $^{15}N$ chemical shift referencing in biomolecular NMR, J. Biomol. NMR 6 (1995) 135–140.
[22] F. Delaglio, S. Grzesiek, G.W. Vuister, G. Zhu, J. Pfeifer, A. Bax, NMRPipe: a multidimensional spectral processing system based on UNIX pipes, J. Biomol. NMR 6 (1995) 277–293.
[23] B.A. Johnson, R.A. Blevins, NMR View: a computer program for the visualization and analysis of NMR data, J. Biomol. NMR 4 (1994) 603–614.
[24] A.S. Stern, D.L. Donoho, J.C. Hoch, NMR data processing using iterative thresholding and minimum l1-norm reconstruction, J. Magn. Reson. 188 (2007) 295–300.
[25] B.A. Cerda, C. Wesdemiotis, Li+, Na+, and K+ binding to the DNA and RNA nucleobases. Bond energies and attachment sites from the dissociation of metal ion-bound heterodimers, J. Am. Chem. Soc. 118 (1996) 11884–11892.
[26] M.T. Rodgers, S.A. Campbell, J.L. Beauchamp, Site-specific lithium ion attachment directs low-energy dissociation pathways of dinucleotides in the gas phase. Application to nucleic acid sequencing by mass spectrometry, Int. J. Mass Spectrom. Ion Process. 161 (1997) 193–216.
[27] N. Russo, M. Toscano, A. Grand, Lithium affinity for DNA and RNA nucleobases. The role of theoretical information in the elucidation of the mass spectrometry data, J. Phys. Chem. B 105 (2001) 4735–4741.
[28] C. Fu, S. Smith, S.G. Simkins, P.F. Agris, Identification and quantification of protecting groups remaining in commercial oligonucleotide products using monoclonal antibodies, Anal. Biochem. 306 (2002) 135–143.
[29] N.M. El Zahar, N. Magdy, A.M. El-Kosasy, M.G. Bartlett, Chromatographic approaches for the characterization and quality control of therapeutic oligonucleotide impurities, Biomed. Chromatogr. 32 (2018), e4088.
[30] J.M. Sutton, G.J. Guimaraes, V. Annavarapu, W.D. van Dongen, M.G. Bartlett, Current state of oligonucleotide characterization using liquid chromatography-mass spectrometry: insight into critical issues, J. Am. Soc. Mass Spectrom. 31 (2020) 1775–1782.
[31] I. Nikcevic, T.K. Wyrzykiewicz, P.A. Limbach, Detecting low-level synthesis impurities in modified phosphorothioate oligonucleotides using liquid chromatography-high resolution mass spectrometry, Int. J. Mass Spectrom. 304 (2011) 98–104.